M-AM-L9

THE ROLE OF THE GANGLIOSIDE G_{D1a} AS A RECEPTOR FOR SENDAI VIRUS. ((R.M.Epand‡, S.Nir|, M.Parolin‡, and T.Flanagan⊥))
‡Dept. of Biochemistry, McMaster University, Hamilton, ON, Canada, L8N 3Z5, |Faculty of Agriculture, Hebrew University, Rehovot 76100, Israel, ⊥Dept. of Microbiology, SUNY, Buffalo, NY 14214.

The ganglioside G_{D1a}, which serves as a receptor for Sendai virus, also affects lipid polymorphism as determined by ^{31}P NMR. The ganglioside promotes the formation of isotropic structures in monomethyl dioleoylphosphatidylethanolamine. G_{D1a} also raises the bilayer to hexagonal phase transition temperature of this lipid. The effects of G_{D1a} on the kinetics of viral fusion can be understood on the basis of its role in facilitating the binding of Sendai virus to target membranes as well as its effects on membrane physical properties. Fusion of Sendai virus with liposomes composed of egg phosphatidylethanolamine is particularly sensitive to the presence of ganglioside. In the absence of ganglioside no fusion is observed due to the absence of virus binding to the target membrane. Between 2 and 6 mol % G_{D1a} in egg phosphatidylethanolamine liposomes there is a marked increase in the rate constant of binding of the virus to the liposomes but a decrease in the fusion rate constant. The ganglioside enhances virus binding to liposomes of all the compositions studied, but the fusion rate constant is either unaffected or reduced. In the systems studied, the enhanced formation of isotropic structures in liposomes containing the gangliosides does not enhance the kinetics of the actual fusion reaction.

LIGHT-DEPENDENT PROTEINS: FUNCTION AND STRUCTURE

M-PM-Sym-1

THE STRUCTURE OF RHODOPSIN OBTAINED BY CRYO-ELECTRON MICROSCOPY TO 7 Å RESOLUTION
((G. F. X Schertler, V. M. Unger and P. A. Hargrave))
All members of the family of G-protein coupled receptors are expected to have the same basic structure in the membrane-embedded part of the protein. Rhodopsin is available from natural sources in reasonable quantities for crystallisation. Two dimensional crystals of bovine and frog rhodopsin have been obtained either by addition of lipids to purified rhodopsin and removal of the detergent or by extraction of frog photoreceptor disk membranes with Tween detergents. Three independent projection structures from bovine $p22_12_1$ and frog rhodopsin p2 and $p22_12_1$ crystals have been obtained. The identity of all three projection maps eliminated any possibility of the structure being affected by crystallisation. A first low resolution 3D structure of bovine rhodopsin was obtained from tilted images of the bovine rhodopsin $p222_1$ crystals (Unger and Schertler Biophys J submitted) and more recently the structure of frog rhodopsin was obtained at improved resolution from the p2 crystal form in three dimensions. In the higher resolution map of frog rhodopsin the tilts of all helices can be deduced. In particular the overall tilt of the more tilted helices is well defined in the frog rhodopsin structure. Baldwin ((1993) EMBO J 12 (4) : 1693-1703) deduced from a detailed analysis of G-protein coupled receptor sequences a set of structural constraints and a possible packing for the helices. These constraints provide an expectation for the environment of each helix and they have been used to make a tentative sequence assignment of the 7 helices in the projection map of bovine rhodopsin (Schertler et al. (1993). Nature 362 (6422) : 770-772). These constraints suggest the possible identity of particular tracks of density now in the 3D-maps of frog and bovine rhodopsin. Helices 1, 2, 3 and 5 are tilted and they form an arc through the center of the molecule. They are flanked by helix 4 on one side, and helices 6 and 7 on the other side, which are approximately perpendicular to the membrane.

M-PM-Sym-2

EXPLORING RHODOPSIN STRUCTURE AND DYNAMICS WITH SITE-DIRECTED SPIN LABELING ((Wayne L. Hubbell[1], Zorheh T. Farahbakhsh[1], Kevin D. Ridge[2], Ke Yang[2], Dave Farrens[2], John Resek[2] and H. Gobind Khorana[2])) [1]Jules Stein Eye Institute and Department of Chemistry and Biochemistry, UCLA, Los Angeles, CA; [2]Departments of Chemistry and Biology, MIT, Cambridge, MA.

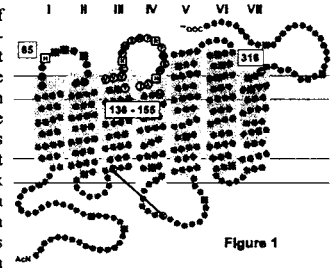

Figure 1

Twenty single-cysteine substitution mutants of rhodopsin in the sequence 136-155, a transducin binding region, and a double mutant containing cysteines at both 65 and 316, were prepared (Fig.1). Each site was modified with a sulfhydryl-specific nitroxide reagent, and the EPR spectra were analyzed. The results demonstrate that: (i) helix III extends to at least residue 140, and ~75% of the helix surface in this region is in contact with protein rather than lipid; (ii) the membrane/solution interface intersects rhodopsin near residues 138 and 152 (Fig. 1); (iii) photoexcitation produces localized changes in tertiary interaction of helix III on a millisecond time scale; (iv) residues 316 and 65, although distant in sequence, are ≤10Å apart in the rhodopsin structure as judged by dipolar interactions between nitroxides at these sites. This demonstrates the close proximity of helices I and VII in the structure, and fixes their relative position along the membrane normal; (v) photoexcitation of rhodopsin results in an increase in distance between 316 and 65, and presumably between helices I and VII. A simple model in which helices III and VII move outward upon deprotonation of the retinal Schiff base accounts for the data.

M-PM-Sym-3

FUNCTION AND STRUCTURE OF REACTION CENTER. ((H. Michel))
Max Planck Inst. for Biophys., Frankfurt.

M-PM-Sym-4

FUNCTIONAL CHARACTERIZATION OF REACTION CENTER MUTANTS.
((C.C. Schenck)) Colorado State Univ.

M-PM-A1

LONG - TERM MODULATION OF Kv1.1 CHANNEL FUNCTION BY PROTEIN KINASE A PHOSPHORYLATION Levin G.*, Keren T.*, Perets T.*, Thornhill W.B.† and Lotan I.*
* Dept. Physiol. & Pharmacol., Sackler School of Medicine, Tel-Aviv University, Ramat-Aviv 69978, Israel. † Dept. Physiol. & Biophys., Mount Sinai School of Medicine, Mount Sinai Hospital, New York, NY 10029-6574.

We have recently[1] characterized , exploiting the Xenopus oocyte expression system, the biosynthesis of the brain Kv1.1 (RCK1) voltage-gated potassium channel and demonstrated that it is a substrate for PKA phosphorylation *in vitro* , is partially phosphorylated *in vivo*, and can be further phosphorylated by a short treatment with a cAMP analog. In this work we study the physiological consequences of the cAMP treatment, by combined two electrode-voltage clamp and SDS-PAGE techniques. It appears that treatments with several cAMP analogs do not affect the channel function. However, a long-term treatment with by a cAMP analog enhances the current amplitude. It also enhance, though, the current amplitude through the channel of which the PKA phosphorylation site is mutated. Concomitant biochemical analysis reveals that the cAMP treatment not only brings about phosphorylation of the wild type channel but also increase the amount of both the wild type and mutant channel proteins. The phosphorylation effect can be separated by the use of a protein synthesis inhibitor; in its presence cAMP enhances mainly the wild-type channel amplitude. We are currently looking into the mechanism underlying this effect.

[1] Ivanina T. et al. Biochemistry 33:8786-8792 (1994)

M-PM-A2

HYDROGEN IONS SHIFT GATING OF AND BLOCK CURRENT THROUGH I_{KS} CHANNELS IN GUINEA PIG VENTRICULAR CELLS BUT NOT I_{MINK} IN HUMAN EMBRYONIC KIDNEY (HEK 293) CELLS. ((Michael Davies and Robert S. Kass)) Department of Physiology, University of Rochester School of Medicine, Rochester, NY 14642.

We investigated the influence of extracellular hydrogen ions on the slowly-activating potassium channel current I_{KS} in guinea pig ventricular cells and on I_{minK} in HEK 293 cells transiently transfected with a synthetic gene encoding the minK channel. Whole cell patch clamp procedures were used to monitor channel activity. Native channels in guinea pig cells were found to be highly sensitive to changes in extracellular pH (pH_o). Relative to pH 7.4, acidification reduced and alkalization enhanced I_{KS} amplitude. Modulation of I_{KS} ranged from 85% reduction (pH 5.0) to a 60% enhancement at pH 10.0. We measured the influence of pH_o on I_{KS} activation threshold and found very large $[H^+]_o$ (pKa=6.5)-dependent gating shifts. $[H^+]_o$-induced alteration in channel gating were not sufficient to account for the influence of $[H^+]_o$ on current amplitude. Data were better described by models incorporating both gating shifts and channel block. Preliminary experiments on the effects of pH_o on I_{minK} expressed in HEK 293 cells indicate that, in these cells, I_{minK} is very insensitive to changes in $[H^+]_o$. Our results show that native I_{KS} channels in guinea pig ventricular cells are very sensitive to $[H^+]_o$, and respond to changes in pH_o differently than minK channels expressed in HEK 293 cells (our results) or in *Xenopus* oocytes (Yamane, et al.,1993). Taken together, these data suggest that interactions of $[H^+]_o$ with the native I_{KS} channel may depend on cellular processing not seen in expression systems into which message for minK alone has been introduced.

M-PM-A3

FUNCTIONAL STOICHIOMETRY: EVIDENCE THAT *MIN K* POTASSIUM CHANNELS CONTAIN TWO *MIN K* MONOMERS. ((Ke-Wei Wang and Steve A. N. Goldstein)) Yale University School of Medicine. Departments of Pediatrics and Cellular and Molecular Pharmacology, Boyer Center for Molecular Medicine, New Haven, CT.

To assess the subunit composition of *min K* potassium channels, the effects of co-expressing wild-type *min K* and a point mutant of the channel, D77N, were studied in *Xenopus laevis* oocytes. Surface expression of both *min K* proteins on individual intact oocytes was measured using an externally exposed epitope tag and monoclonal antibodies; *min K*-induced potassium channel currents were measured by two-electrode voltage clamp. Surface expression of wild-type and D77N *min K* molecules is found to be random and unbiased. Although D77N-*min K* is expressed on the cell membrane in a fashion identical to wild-type, it is a null mutation which passes no current. Injecting a constant amount of wild-type cRNA with increasing amounts of D77N cRNA leads to decreased potassium current. Residual current appears wild-type in both its potassium selectivity and gating kinetics. This suggests that the two molecules interact to form non-functional multimeric complexes and that only fully wild-type channels conduct ions. A simple binomial distribution was applied to analysis of the current resulting from mixing of the two subunit types. Current was fit best by a model with two wild-type *min K* monomers per functional potassium channel. A non-*min K* protein also appears to be required for channel function since current saturates despite increasing levels of wild-type *min K* on the cell membrane.

M-PM-A4

THE CONDUCTANCE OF MinK 'CHANNELS' IS VERY SMALL. ((Y. Yang and F. J. Sigworth)) Cellular and Molecular Physiology, Yale Univ. School of Medicine, New Haven CT 06510.

From *Xenopus* oocytes expressing the rat MinK message, some inside-out macropatches display a small, slowly-activating K-selective conductance. Like the patch recordings of cardiac myocyte I_K by Walsh et al. (*Am. J. Physiol.* 260: H1390, 1991) the time course of activation is very smooth, with no visible single-channel behavior (A). Subtraction of pairs of responses from 40 s depolarizations to +50 mV leaves very small residuals (B). The 'power spectrum' of the nonstationary fluctuations (Sigworth, *Biophys. J.* 35:289, 1981) has a constant component of the magnitude expected for shot noise from ion transport, plus a $1/f^2$ component consistent with Wiener-Lévy noise from stepwise increases in conductance during the depolarization. The calculated elementary step size is ~0.3 fA, a 'single channel' current corresponding to ~2000 ions transported per second.

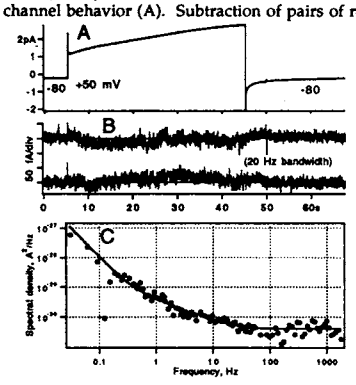

M-PM-A5

MIN K DOES NOT SPECIFICALLY ACTIVATE ENDOGENOUS CHLORIDE CHANNELS IN *XENOPUS* OOCYTES. ((T. Tzounopoulos, J. Maylie and J. Adelman)), Oregon Health Sciences University, Portland, OR 97201.

Min K, a protein of 130 amino acids with a single transmembrane domain, induces a slowly activating voltage-dependent potassium current when expressed in *Xenopus* oocytes. Mutations within the transmembrane domain altered ion selectivity suggesting that min K is a channel-forming protein (Goldstein *et al*, Neuron 2, 403-408, 1991). However, recent data (Attali *et al*, Nature 365, 850-852, 1993) report that high levels of min K expression in *Xenopus* oocytes also induce a DIDS-sensitive chloride current with biophysical and pharmacological characteristics very different from those of the min K induced potassium current. These data have been interpreted in a model in which min K activates endogenous, otherwise silent potassium and chloride channels. Here, we report that high levels of expression of several structurally unrelated membrane proteins in *Xenopus* oocytes results in the induction of a similar chloride current. A hyperpolarization-activated inward chloride current was observed with high levels of expression of a glutamate transporter (EAAT2), a nonconducting voltage-dependent potassium channel (Shaker W434F), a nonconducting inward rectifier potassium channel (BIR9) and min K. This current showed very slow activation kinetics, with a threshold potential near -80 mV. Additionally, the current was reduced 50% by DIDS (0.5 mM). We conclude that this chloride current is not specific for min K but appears as a result of high expression of membrane proteins in *Xenopus* oocytes. Consequently, min K can not be considered as a regulator of endogenous silent potassium or chloride channels based on the induction of this hyperpolarization-activated inward current.

M-PM-A6

MOLECULAR BASIS OF PEROXIDE AND MERCURY MEDIATED I_{SK} REGULATION ((A.E. Busch*, T. Herzer*, S. Waldegger*, C.A. Wagner*, E. Gulbins*, T. Takumi$, K. Moriyoshi#, S. Nakanishi# and F. Lang*)) Physiological Institute, Eberhard-Karls-University Tübingen*, Germany; Faculties of Medicine of the Osaka University$ and Kyoto University#, Japan. (Spon. by R. Rahamimoff)

Expression of the I_{sK} protein in *Xenopus* oocytes or HEK 293 cells induces slowly activating potassium currents, although it is structurally and functionally distinct from other potassium channel proteins. In heart, the I_{sK} protein mediates the potassium conductance I_{Ks}. Since inhibition of I_{Ks} by peroxides may be involved in the genesis of reperfusion-induced arrhythmias, the influence of oxidation on I_{sK} channels was investigated. Here we show inhibition of I_{sK} expressed in *Xenopus* oocytes by membrane permeable oxidative agents, while no inhibition was observed for I_{sK} protein mutants carrying a Ser-mutation instead of a highly conserved intracellular Cys-residue. In contrast, Hg^{2+}, which may not only oxidize thiol-groups but also form chelates with dibasic amino acids, caused a use-dependent, persistent activation of I_{sK}, as previously found for extracellularly acting organic cross-linkers. This effect was not influenced by the intracellular Ser-mutation but was reversed in an I_{sK} protein mutant with a deletion in the extracellular domain. These data suggest that the intracellular redox-potential controls I_{sK} activity and that activation of I_{sK} channels involves an approximation of the extracellular protein tail.

M-PM-A7

HYPERPOLARIZATION ACTIVATED CURRENT (I_h) AND ITS MODULATION IN MAMMALIAN RETINAL RODS. ((G.C. Demontis and L. Cervetto)) Istituto Policattedra di Discipline Biologiche, Università di Pisa, 56126 Pisa, ITALY.

Voltage activated currents where measured from the inner segment of isolated guinea-pig rods by the whole-cell voltage clamp method. I-V curves obtained by stepping the voltage from a holding potential of -30 mV (close to the dark membrane potential of the cell) showed both inward and outward rectification. Membrane hyperpolarizations up to -130 mV, at room temperature, activated a slow inward component with a time constant of about 300 ms. The hyperpolarization activated current (I_h) displayed a steep voltage dependence as shown by fitting the tail currents, measured at -60 mV, by a Boltzmann relation with a half-activating voltage of -87 mV ± 9.8 mV (S.E.M.) and a slope factor of 10 mV ± 1.7 mV. The ionic selectivity was determined by fitting the I-V measurements by a GHK equation with the Na/K permeability of 0.35 ± 0.03. I_h activation was unaffected by 1 mM Co^{++}, 1 mM Ba^{++} and 30 mM TEA. Complete blockage of I_h was obtained by application of 5 mM Cs^+ or 200 μM zatebradine. Application of a membrane permeant analog of cAMP shifted the I_h activation curve to a less negative voltage with no effect on the slope factor. As opposed to cAMP, micromolar concentrations of dopamine reversibly shifted the I_h activation curve to more negative voltages. This effect was prevented by priming the visual cell in a solution containing 10 μM clozapine, a specific inhibitor of dopamine receptors. These results suggest that the voltage gated I_h channels of retinal rods are modulated by dopamine through adenylyl cyclase inhibition.

Supported by CNR and MPI 60% grants to L.C.

M-PM-A8

PREFERENTIAL BLOCKADE OF I_H IN RAT TRIGEMINAL GANGLION NEURONS BY DK-AH 268 ((D. Janigro, M.E. Martenson* and T.K. Baumann*)) Depts. of Neurosurgery Univ. of Washington, Seattle, WA and Oregon Health Science University, Portland, Ore*

Hyperpolarization-activated cation currents (I_h or I_H) are believed to control neuronal excitability. Selective blockers of h-type currents are not available. Cesium and rubidium ions block I_h, but both also strongly interfere with inward potassium currents. We tested the specificity and potency of a novel organic I_h current blocker in voltage clamped cultured rat trigeminal neurons. In these neurons, negative voltage clamp steps (from -40 mV) elicited large I_h currents. Low concentrations (10 μM) of the putative I_h blocker DK-AH 268 (DK, Boehringer), caused a 30% reduction of I_h. This effect was selective for I_h since outward potassium currents elicited from the same potential were unaffected. Current subtraction protocols revealed that the currents blocked by DK (10 μM) or external Cs^+ (3 mM) had virtually identical voltage- and time-dependent activation properties suggesting that DK and Cs^+ caused blockade of the same current. Time-independent, inwardly rectifying currents were unaltered by 10 μM DK. At higher concentrations of DK (100 μM) a more pronounced block of I_h and a decrease in specificity were observed. Blockade of I_h appeared to be use-dependent since it required membrane hyperpolarizations. Relief of DK block was also aided by hyperpolarization. Since both DK-and Cs-sensitive time-dependent currents behaved as I_h, we conclude that 10 μM DK can selectively reduce I_h without affecting potassium currents. Thus, DK may be an useful agent in the investigation of I_h current function (supported by NIH NS 51614, NSF IBN 94-12518, and the National Headache Foundation).

K^+ CHANNEL VESTIBULES

M-PM-B1

AN INHIBITOR OF THE KV2.1 K^+ CHANNEL ISOLATED FROM GRAMMOSTOLA SPATULATA VENOM. ((Kenton J. Swartz and Roderick MacKinnon)) Dept. of Neurobiology, Harvard Medical School, Boston, MA 02115.

The Kv2.1 K^+ channel (drk1) is insensitive to a variety of K^+ channel inhibitors, including charybdotoxin, agitoxin and dendrotoxin. We have isolated two inhibitors of the Kv2.1 K^+ channel from the venom of the *Grammostola spatulata* spider using reverse phase HPLC and a screening procedure that involves the expression of the cloned K^+ channel in *Xenopus* oocytes. These inhibitors have no sequence homology to other known K^+ channel inhibitors. They are 35 residue peptides that contain six cysteines, and differ only by a single residue at position 13. We designated the isoform with serine at position 13 as hanatoxin$_1$ and the isoform with alanine at position 13 as hanatoxin$_2$. These two isoforms are difficult to separate when folded, but can be separated following reduction with dithiothreitol. Hanatoxin$_1$ was synthesized using both recombinant and solid phase chemical methods. Both methods yield active peptide, but only in very low yield (1-3%). We are currently studying the mechanism of hanatoxin-induced inhibition of the Kv2.1 K^+ channel.

M-PM-B2

THE MOLECULAR PICTURE OF THE α-DENDROTOXIN BINDING SITE ON A MAMMALIAN K CHANNEL. ((J. Tytgat*† and E. Carmeliet*)) Laboratory of Physiology*, Laboratory of Toxicology†, University of Leuven, Leuven 3000, Belgium.

α-Dendrotoxin (α-DTX), a 59 amino acid basic peptide from *Dendroaspis angusticeps* belonging to the family of mamba snakes, potently blocks RBK1 channels by interacting with the amino acid segment between transmembrane domains S5 and S6 (IC_{50} 1 nM (Hurst *et al.* (1991) Mol. Pharmacol. 40:572-576)). The same authors have shown that mutation of three residues in RBK1 (Ala352, Glu353 and Tyr379), to match the equivalent positions in α-DTX-insensitive RGK5 channels (Pro374, Ser375 and His401), causes a ≈150-fold decrease in the α-DTX sensitivity. To investigate the specific mechanism of α-DTX interactions with α-DTX-sensitive RCK1 channels, we have made the same mutations (Ala352Pro, Glu353Ser and Tyr379His) and constructed tetrameric cDNAs in one open reading frame composed of different combinations of wild-type (WT) and mutant subunits. IC_{50}-values for block by extracellularly applied α-DTX in homomeric WT and mutant RCK1 channels were 1.1 and 199.3 nM, respectively. IC_{50}-values for heteromeric channels with 3:1, 2:2 and 1:3 WT and mutant subunits were 5.1, 17.6 and 84.4 nM, respectively. These results show a linear relationship between the free energy for α-DTX binding and the number of WT subunits. We conclude therefore that all four subunits must interact simultaneously with an α-DTX molecule to produce a high affinity binding site. A similar mechanism of additive contributions from all four subunits has also been shown for the external TEA binding site in *Shaker*-type K channels (Heginbotham and MacKinnon (1992) Neuron 8:483-491; Liman *et al.* (1992) Neuron 9:861-871).

M-PM-B3

TOPOLOGICAL MAP OF THE RECEPTOR SITE FOR IMMUNOSUPPRESSIVE PEPTIDES ON A LYMPHOCYTE K^+ CHANNEL, Kv1.3 ((J. Aiyar, J. Rizzi, J. Withka, C-L Lee, G. Andrews, B. Dethleffs, M. Simon, G.A. Gutman and K. G. Chandy)) Dept. of Physiology & Biophysics UCI, Irvine, CA 92717 and Dept. of Computational Chemistry, Pfizer Inc., Groton, CT. 06340.

Kv1.3 modulates the immune response. Peptide blockers of Kv1.3, are effective immunosuppressants. Here we describe the molecular interactions responsible for the binding of four such structurally related peptides, kaliotoxin (KTX), charybdotoxin (ChTX), noxiustoxin (NTX), and margatoxin (MgTX), to their receptor within a vestibule on the external surface of the Kv1.3 pore; these peptides are held in a rigid conformation by three disulfide bonds. Mutation studies of Kv1.3 identified three channel residues D386, H404, G380, that were critical for KTX block. By examining the effects of peptide mutants, we were able to demonstrate the following KTX-channel interactions: R24-D386, F25-H404, L15 and R31 with opposing G380s. Knowing the distance between these KTX residues we estimated the dimensions of the vestibule. An additional reference point is K27 which possibly interacts with D402 in the pore. D386 is ~7-9Å from H404 (based on distance between R24 to F25), ~11-13Å from the center of the pore (R24 to K27), and ~22-26Å from the opposing D386 (assuming a symmetrical homotetramer). H404 is 4-6Å from the center of the pore (R25 to K27) and ~8-12Å from H404 in the opposing subunit. The vertical depth of from D386 to G380, is ~4-6Å, based on the distance from R24 to L15. The outer mouth of the vestibule in the homotetramer is limited by the positions of the G380s. Replacing G380 (r = 2.5Å) with E (r = 3.2Å) converts a KTX-sensitive channel to one that is resistant; the outer mouth is therefore between 25Å (size of KTX) and 26.5Å (KTX + 2X difference between the radii of G and E).

M-PM-B4

MAPPING THE INTERACTION SURFACE OF THE PORE-BLOCKING K^+ CHANNEL INHIBITOR AGITOXIN 2. ((Rama Ranganathan, John H. Lewis, Roderick MacKinnon)) Department of Neurobiology, Harvard Medical School, 220 Longwood Ave., Boston, MA 02115. (Sponsored by Bruce P. Bean)

The scorpion toxin Agitoxin 2 (AgTx2) blocks ion permeation through Shaker K^+ channels by direct, high-affinity binding to the external pore region. High-resolution 3-D structure of the toxin protein reveals a highly rigid backbone architecture organized into an α-helix resting on two β-strands forming a tight anti-parallel hairpin. Toxin residues making specific interactions with the pore of the channel (K27) and with channel residue D431 (R24 and R31) fall on one of the β-strands, suggesting that residues in this region may travel along the channel surface immediately surrounding the pore. We have now carried out an alanine-scanning mutagenesis of AgTx2 and show that in fact other residues in this region (F25, M29, N30) contribute significantly to the overall binding energy. Thus, this β-strand forms an important part of the toxin interaction surface. The analogous region in charybdotoxin, an AgTx2 isoform, also interacts with the Shaker K^+ channel (Goldstein, Pheasant, and Miller; Neuron 12:1377), although the binding energies of individual residues vary greatly. A spatial mapping of the residues forming this surface onto the pore forming segment of the Shaker K^+ channel should provide important structural constraints on the topology of the external ion permeation pathway.

M-PM-B5

THERMODYNAMIC MUTANT CYCLES WITH THE SHAKER K+ CHANNEL AND AGITOXIN2 DEFINE THE SPATIAL LOCATION OF PORE-FORMING RESIDUES. ((Patricia Hidalgo and Roderick MacKinnon)) Department of Neurobiology, Harvard Medical School, Boston, MA 02115.

Agitoxin$_2$ was used as a structural template to determine the spatial arrangement of amino acids forming the P-region of the *Shaker* K+ channel. Paired interactions between channel and toxin amino acids were identified through the introduction of point mutations on both proteins. The mesaurement of four inhibition constants corresponding to wild type toxin/wild type channel ($K_{WT:WT}$), mutant toxin/wild type channel ($K_{Mut:WT}$), wild type toxin/mutant channel ($K_{WT:Mut}$) and mutant toxin/mutant channel ($K_{Mut:Mut}$) define a thermodynamic cycle. Deviation of the quantity $\Omega = (K_{WT:WT} * K_{Mut:Mut}) + (K_{WT:Mut} * K_{Mut:WT})$ from unity signifies a coupled interaction between the pair of residues under study. A large data set corresponding to many residue pairs allows one to determine whether the coupling occurs through a local interaction. We show that Asp 431 residues on diagonally-opposed channel subunits interact with Arg 24 and Arg 31 on opposite sides of Agitoxin$_2$. Arg 24 appears to interact through an ionized hydrogen bond while Arg 31 interacts by a through-space electrostatic mechanism. These findings constrain the amino-terminal extent of the P-region to be located 11 Å to 14 Å from the central axis of the pore.

M-PM-B6

COUNTING POINTS OF INTERACTION BETWEEN A *Shaker* K+ CHANNEL VESTIBULE AND A PEPTIDE TOXIN. ((D. Naranjo and C. Miller)). HHMI and Graduate Department of Biochemistry, Brandeis U., Waltham, MA 02254.

Charybdotoxin (CTX) is a 37 amino acid peptide with known three-dimensional structure that binds selectively to the external vestibule of K+ channels. CTX, whose structure does not reveal apparent structural symmetry, can interact in four equivalent orientations with the symmetrical tetrameric *Shaker* channel. Thus, in a given orientation of binding, the toxin is not interacting with four equivalent channel residues in the same manner. We present a methodology to determine how many, of four equivalent, residues of the channel interact with the toxin once it is bound. We make use of two *Shaker* mutants with a single amino acid difference in the external vestibule (449T and 449F), but with a 10000-fold difference in affinity for the M29I mutant of CTX. Mixtures of cRNA encoding for these two *Shaker* variants were injected at various ratios into *Xenopus* oocytes and their expression was examined with two electrode voltage clamp. 10 nM of M29I-CTX, a concentration 100-fold above the dissociation constant (K_d) for 449T-*Shaker* and 100-fold below the K_d for 449F-*Shaker*, was applied to the bath and the kinetics of toxin unbinding was studied. The fractional blockade gets more intense as the molar fraction of the injected cRNA for the 449T variant is increased. In general, the unbinding kinetics follows a clear bi-exponential time course with time constants of ~30 and ~600 sec. For molar fraction of 449T cRNA < 0.15 the fast component of the unbinding is prominnent, however for molar fraction > 0.4 the unbinding only show the slow component. Assuming binomial distribution of these two *Shaker* mutant subunits, we can estimate that the toxin's residue 29 interact closely with residues 449 of two adjacent subunits of the channel. With these results is possible to make definite prediction on the geometry of the channel-toxin interaction.

M-PM-B7

PROBING THE MOUTH OF A K+ CHANNEL WITH SH-REAGENTS OF DIFFERENT DIAMETER AND CHARGE AFTER CYSTEINE-SCANNING MUTAGENESIS. ((H-J., Zhang, Y. Liu, R.D. Zühlke, L.L. Kürz and R.H. Joho)) Department of Cell Biology and Neuroscience, The University of Texas Southwestern Medical Center, Dallas, TX 75235-9111.

The segment between S5 and S6 of voltage-gated K+ channels has been implicated to form part of the ion conduction pathway. Little is known about the conformation of this region although various models have been proposed. To gain insight into the secondary structure of this region, we used cysteine-scanning mutagenesis and sulfhydryl-specific, membrane-impermeant reagents of different diameter and charge to probe side-chain accessibilities of mutated amino acids in the pore region of Kv2.1 (DRK1). We previously identified several positions that, when mutated to cysteine, showed current reduction after superfusion with the small Cd^{2+} ion as well as the larger 6x10 Å methanethiosulfonate-derivative MTSET. These results suggested that the side chains of K356C, P361C, I379C, Y380C, and K382C were directly accessible from the extracellular environment, presumably facing the aqueous lumen of the ion channel pore. Mutant I379C exhibited the largest reduction (>95%) of current amplitude, suggesting that position 379 may be in a narrow part of the pore. To explore the molecular dimensions at position 379 of Kv2.1, we have begun to study the effects of several sulfhydryl-specific reagents of different diameter and charge. Coupling positively or negatively charged MTS-derivatives leads to similar current reduction, suggesting that steric hindrance but not electrostatic effects plays a major role at position 379. Currently, we are testing several SH-specific reagents of smaller diameter in an attempt to uncover additional positions in the deep part of the ion conduction pathway. (Supported by grants from the NIH and MDA [RHJ] and the Am. Heart Assoc./Texas Affiliate [HJZ].)

M-PM-B8

SIDE-CHAIN EXPOSURE IN THE P-REGION OF A CYSTEINE-SUBSTITUTED K+ CHANNEL PROBED BY SILVER CATION. (Q. Lu and C. Miller) HHMI, Graduate Dept. of Biochemistry, Brandeis University, Waltham, MA.

The major ion selectivity determinants of K+ channels are found in a short stretch of contiguous residues, the P-region. We have substituted cysteine at each P-region position of a *Shaker* K+ channel (positions P430-P450, numbered P0-P20 here) and challenged these channels with an inorganic thiol-labelling reagent, Ag^+. We expressed in *Xenopus* oocytes mixed-subunit channels containing a single cysteine in the *Shaker* tetramer. In this way, 20 of the 21 constructs expressed K+ channels with conventional voltage-dependent kinetics. Upon application of 200 nM Ag^+ to the external solution, channels substituted at certain positions were inhibited irreversibly in several minutes. Channels bearing cysteine at other positions were unaffected. Shaded residues project side-chains into the aqueous pore lumen or external vestibule. Unshaded residues are Ag^+-insensitive and project side-chains backwards into the protein mass. Hatched residues are, for various reasons, equivocal in interpretation. Our main conclusions are (1) that the narrower part of the pore is lined by residues in the sequence W4-M18, and (2) that the pattern of Ag^+ accessibility is inconsistent with a β-barrel structure of the pore.

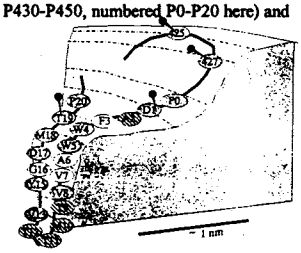

M-PM-B9

THE AGITOXIN FOOTPRINT ON THE *SHAKER* POTASSIUM CHANNEL. ((Adrian Gross and Roderick MacKinnon)) Department of Neurobiology, Harvard Medical School, Boston, MA 02115.

Agitoxin$_2$, a peptide inhibitor, binds to the pore region of the *Shaker* channel with 1:1 stoichiometry. Since the asymmetric toxin binds to a four-fold symmetric channel, we can distinguish three classes of channel residues: (1) central residues, covered by toxin on all four subunits, (2) residues covered on 1-3 subunits, and (3) residues not covered at all. We have used two independent techniques to map residues in the toxin binding site (the S5-S6 linker) to one of these three classes.

First, we substituted lysines at all positions in the S5-S6 linker, except the highly conserved P-region. The closer to the binding site we introduce a positively charged residue, the more the positively charged toxin is repelled. Residues outside the binding site (class 3) affect mainly the toxin on-rate, whereas residues in the binding site (class 1 and 2) also affect the off-rate. To distinguish between classes 1 and 2, we introduced the lysine in only one of the four subunits using the inactivation gate as a tag. Second, we substituted cysteines into the binding site and studied whether they could be chemically modified in the presence of toxin. (By definition, a class 1 residue cannot be modified in the presence of toxin.) We conclude that T449 is a class 1 residue located close to the channel pore. This finding is in agreement with previous studies on TEA binding. Residues F425, D431, V451 are class 2 residues that lie outside the core shadow of the toxin.

M-PM-C1

HALF-THE-SITES PHOTOINACTIVATION OF RHO PROTEIN SUPPORTS THE FUNCTIONAL DIMER MODEL. ((S. Swenson, L.K.F. Lau and S.E. Seifried)) Department of Biochemistry and Biophysics, University of Hawaii, Honolulu, HI 96822.

E. coli transcription termination factor rho has an NTPase activity necessary for its biological function. Hydrolysis of the β-γ bond of nucleoside triphosphates is required for translocation along the nascent RNA and the ultimate termination function. The hexameric protein is organized as a trimer of dimers. Each identical subunit contains an NTP binding site. The functional dimer model predicts the inactivation of an NTP binding site on one of the two monomers in the functional dimer to inactivate the entire dimer. Through the use of s^4UTP, a photoaffinity ATP analogue, we have identified the number of functional binding sites required for the NTPase activity. We have correlated the number of NTPs bound to levels of NTPase activity. This has allowed the construction of a model that describes the parameters under which NTP is bound and hydrolyzed. These findings support the functional dimer model and disallow some alternate models. Further studies will elucidate the kinetics of NTP binding, hydrolysis, and product release, and the physical relationship between rho and RNA.

M-PM-C2

PROTEIN-DNA INTERACTIONS OF THE ALPHA SUBUNIT OF RNA POLMERASE ((Heyduk, E. and Heyduk, T.)) Department of Biochemistry and Molecular Biology, St. Louis University School of Medicine, St. Louis, MO 63104

Regulation of *E. coli* RNA polymerase (RNAP) involves a complex array of inter- and intramolecular communications. It has been established for a long time that recognition of -10 and -35 promoter elements is accomplished by a sigma subunit of RNA polymerase. Recently, the alpha subunit has been shown to interact specifically with AT rich sequences upstream the core promoter sequences.[1] This interaction leads to a pronounced activation of RNAP. Here we present data reporting the thermodymanics of this interaction. Binding of alpha to 41 bp DNA fragment containing the alpha binding site from *rrnB*P1 promoter was investigated. Stoichiometry, salt and temperature dependence of the binding was determined. Protein regions involved in DNA binding were identified using protein footprinting approach.[2] The importance of these results with respect to understanding the mechanism of RNAP activation will be discussed.

1. Ross, W., Gosink, K.K., Salomon, J., Igarashi, K., Zou, C., Ishihama, A., Severinov, K. and Gourse, R. *Science* **262**, 1407-1403, 1993
2. Heyduk, E. and Heyduk, T. *Biochemistry* **33**, 3643-3650, 1994.

M-PM-C3

Real-Time BIAcore Measurements of Escherichia coli Single-Stranded DNA Binding (SSB) Protein to Polydeoxythymidylic Acid
((Robert J. Fisher,Matthew Fivash,Jose Casas-Finet,Sharon Bladen,and Karen Larson McNitt)) NCI-FCRDC, Frederick, MD 21702 (Spon. A.E. Shamoo)

The Pharmacia BIAcore® Biosensor was used to measure the real-time interaction of *Escherichia coli ssb* protein with polydeoxythymidylic acid. This approach may have general applicability in the design and analysis of BIAcore® binding experiments. A streptavidin chip is modified with three different surface densities of biotinylated oligonucleotide and a fourth channel is modified only with streptavidin. This allows examination of collected data for surface crowding effects, for flow limiting or reaction limiting binding, and for surface saturation. These observations are used to develop a mathematical model to describe the family of sensorgrams from a series of surface densities and protein concentrations with a single set of parameters. Thus a series of sensorgrams from three different surface densities of DNA and three orders of magnitude *ssb* concentraton are solved from washon through washout phase. The model presented is consistent with kinetic data for the association and dissociation rate constants for *E. coli ssb* and permits calculation of a thermodynamic binding constant. The concept of steric cooperativity is introduced to explain the observed increasing rate of binding as the surface binds more *ssb* protein. A complementary method for the measurement of a model independent thermodynamic binding constant in the BIAcore® is also presented.

M-PM-C4

FLUORESCENCE STUDY OF INTERACTIONS BETWEEN THE VP16 ACTIVATION DOMAIN AND BASAL TRANSCRIPTION FACTORS TBP AND TFIIB. ((Fan Shen*, Steven J. Triezenberg*, Preston Hensley+, Denise Porter# and Jay R. Knutson#)) *Dept. of Biochemistry, Michigan State Univ., East Lansing MI 48824, +Dept. of Macromolecular Sciences, SmithKline Beecham, King of Prussia PA 19406, and #NHLBI, LCB, NIH, Bethesda MD 20892.

The HSV-1 virion protein, VP16, is a potent transcriptional activator of viral immediate early genes. The activation domain resides in the C-terminal 78 amino acids (413-490). Mutational analyses of this domain have indicated that specific aromatic and hydrophobic amino acids are important for its function. Biochemical analyses have suggested that the VP16 activation domain can interact with components of the basal transcriptional machinery (e.g. TBP or TFIIB) to activate transcription. However, little is known about structure of this domain or the mechanism by which it interacts with these proteins. We initiated fluorescence analysis employing chimeric proteins comprising the GAL4 DNA-binding domain (1-147) fused to the VP16 activation domain. Trp residues were substituted for Phe at either 442 or 473 of VP16, thus providing unique fluorescence probes at two positions. Dynamic quenching, time-resolved fluorescence decay and time-dependent anisotropy decay studies showed that the Trp residues at either position are solvent exposed and highly mobile. To examine the interactions between VP16 and its potential targets, TBP and TFIIB, we incorporated 5-hydroxy-Trp or 7-aza-Trp at 442 or 473 of VP16. Their fluorescence can be selectively excited in complexes with other Trp-containing proteins. Steady-state anisotropy titration studies provided the equilibrium binding parameters. The 7-aza-Trp residues at either position showed a spectral shift in the presence of TBP (but not TFIIB), indicating a change to a more hydrophobic environment. In anisotropy decay experiments using 5-hydroxy-Trp at either position, TBP induced a more ordered structure in the VP16 domain. In contrast, TFIIB induced only a slight change and only for VP16 labeled at 473. Our results support previous models of TBP as a target protein for transcriptional activators and suggest that folding of the VP16 activation domain is induced upon interaction with target proteins.

M-PM-C5

STRUCTURE AND DNA-BINDING OF A THERMOSTABLE PROTEIN FROM *SULFOLOBUS SOLFATARICUS*. ((H. Baumann, S. Knapp, T. Lundbäck, A. Karshikoff, R. Ladenstein and T. Härd)) Center for Structural Biochemistry, Karolinska Institutet, NOVUM, S-141 57 Huddinge, Sweden.

We have determined the structure of a small basic and abundant DNA-binding protein (Sso7d) from the archaeon *Sulfolobus solfataricus* using nuclear magnetic resonance (NMR). The Sso7d protein consists of a triple-stranded anti-parallel β-sheet onto which an orthogonal double-stranded β-sheet is packed. The structure is very similar to that of eukaryotic SH3 domains, suggesting that this folding motif has been conserved in the two kingdoms due to its (thermal) stability. The binding of Sso7d to various polynucleotides was characterized using tryptophan fluorescence spectroscopy. Sso7d binds strongly (K_d < 10μM) to double stranded DNA sequences and Sso7d binding increases the T_m of DNA by as much as 39°C. NMR was used to identify the DNA-binding surface of Sso7d. Calculations of electrostatics show that the identified DNA-binding surface has a strong positive potential, as expected. Five lysine residues in the Sso7d protein are specifically subjected to ε-mono-methylation in the cell. The extent of methylation is dependent on cell growth temperature, suggesting a role in the response of the organism to heat shock. The methylated lysine side chains are located opposite to the DNA-binding surface, consistent with a methylation of Sso7d in complex with DNA. A possible biological function of Sso7d is to protect the genetic material in *Sulfolobus* (living at temperatures around 80°C) from thermal denaturation.

M-PM-C6

DYNAMIC RECOGNITION ELEMENTS IN THE TBP-TATA BOX INTERACTION. ((N.Pastor and H.Weinstein)) Dept. Physiol. and Biophys., Mt. Sinai School of Med., New York, NY 10029. (Sponsored by M.Sassaroli)

Transcription of many mRNAs starts with the binding of a TATA-box Binding Protein (TBP) to a DNA sequence, known as the TATA box (consensus T A T A T/A A A), located 30 base pairs upstream of the start site. The direction of binding of the asymmetric TBP molecule to DNA is important because it determines the direction of transcription. Because TBP binds in the minor groove where AT and TA base pairs present very similar groups for recognition, the determinants for the directionality must relate to another property of the sequence. The flexibility of the DNA has been suggested as such a determinant, because the 5' end of the TATA box, consisting of alternating pyrimidine-purine DNA, is thought to be more flexible than the 3' end, which is an A-tract and is considered to be rigid. To ascertain the role of flexibility in determining the direction of TBP binding, we carry out molecular dynamic simulations of six DNA dodecamers containing TATA box sequences. The simulations are done with the CHARMM22 potential, using periodic boundary conditions, explicit water (TIP3) and one sodium ion/DNA phosphate. The sequences studied are the consensus sequences, an inverted TATA box, and two specificity mutants, all of which can promote transcription *in vitro*. A sequence where AT base pairs were changed to IC is included to test the structural and dynamic equivalence of these base pairs. Measures of local flexibility and sequence-dependent conformation are used to extract from the simulations a set of discriminant properties of these sequences, and to evaluate their effect on TBP complexation.

Supported by a Fulbright/CONACyT fellowship (NP), and by the Assoc. for Intl. Cancer Research.

M-PM-C7

CHARACTERIZATION OF THE DYNAMICAL STRUCTURE OF A PROTEIN-DNA COMPLEX: THE λ-REPRESSOR-OPERATOR

((S. Vijayakumar, G. Ravishanker and D. L. Beveridge)) Department of Chemistry, Wesleyan University, Middletown, CT 06459.

Understanding the specificity of a regulatory protein to it's cognate DNA sequence requires detailed characterization of the underlying interactions and interpretive knowledge of the relative contributions leading to the overall stability. We report herein details of the dynamical structure of the repressor protein from phage λ, its cognate DNA sequence (OL1) and that of the repressor-operator complex. This system is of historic interest in the elucidation of the 'genetic switch' from lysogenic to lytic phases of the phage λ, has been studied extensively from diverse points of view, and forms a suitable basis for inquiring into the overall credibility, accuracy and utility of MD simulation applied to a regulatory protein-DNA complex. Separate simulations of the repressor protein, DNA and that of the complex were carried out in a box of SPC waters using the GROMOS force field starting from the x-ray coordinates of the complex. The results were examined for the intrinsic flexibility of the operator DNA, the repressor and any conformational changes that occur on complex formation. The dynamical structure is also analyzed in terms of existing theories on DNA bending.

M-PM-C8

SPECTROSCOPIC IDENTIFICATION AND MAPPING OF PROTEIN AND DNA BY SOFT X-RAY MICROSCOPY.

((X. Zhang, C. Jacobsen, J. Kirz, S. Williams*)) Physics Department, SUNY, Stony Brook NY 11794-3800 and ((R. Balhorn)) Lawrence Livermore National Laboratory, Livermore, CA 94550.

Details of resonant structures near x-ray absorption edges (XANES) are characteristic of the chemical environment of the absorbing atom. In scanning soft x-ray microscopy it is possible to obtain spectra from submicron areas, and to use these spectral features to map the distribution of dominant constituents of specimens such as proteins and DNA. We have applied this method to the study of chromosomes, fibroblasts, and sperm from several species. The resolution is about 50 nm. The specimens used so far have been dry, although we are also able to image wet specimens. Our aim is to extend this method to frozen hydrated specimens, and to the mapping of lipids and carbohydrates in addition to protein and DNA. The high penetrating power of soft x-rays should make it possible to examine whole, unsectioned specimens through ice layers up to 10 μm thick.

* present address, Department of Molecular Biophysics and Biochemistry, Yale University, New Haven, CT 06510

MEMBRANE ASSEMBLIES

M-PM-D1

STRUCTURE OF PHOSPHOLAMBAN RECONSTITUTED IN SUPPORTED BILAYERS FROM FTIR SPECTROSCOPY

((Suren A. Tatulian, Larry R. Jones†,Laxma G. Reddy, David L. Stokes, and Lukas K. Tamm)) Dept. of Mol. Physiology and Biol. Physics, Univ. of Virginia School of Medicine, Box 449, Charlottesville, VA 22908, and †Krannert Institute of Cardiology, Indiana Univ. School of Medicine, Indianapolis, IN 46202

The secondary structure and the spatial orientation of native phospholamban (PLB), a 52-residue integral membrane protein that regulates calcium uptake into the cardiac sarcoplasmic reticulum, as well as of its 27-residue C-terminal transmembrane segment (PLB_{26-52}), reconstituted in DMPC bilayers, were determined using polarized attenuated total reflection (ATR) Fourier transform infrared (FTIR) spectroscopy. The major component of the amide I' bands of PLB and PLB_{26-52} was centered at 1654-1657 cm^{-1} and was assigned to α-helix. The fraction of α-helix in native PLB was 63 % (~33 residues); the peptide PLB_{26-52} contained 72 % α-helix (~20 residues). Small fractions of β- and random structures were also identified. The orientational order parameter (S) of the α-helical component of PLB_{26-52} was $S = 0.86 \pm 0.09$, indicating that the transmembrane helix was oriented approximately perpendicular to the membrane plane. The additional α-helical residues in PLB were assigned to the cytoplasmic helix and determined to have an order parameter $S = -0.15 \pm 0.30$ implying an oblique orientation of the cytoplasmic helix. PLB was phosphorylated in the supported bilayers by protein kinase A, as confirmed by the appearance of a new absorbance band at ~1200 cm^{-1}. Phosphorylation reduced the α-helical content of PLB to 54 % (~28 residues), though the orientation of the cytoplasmic helix was not significantly changed. These results, in conjunction with a Chou-Fasman secondary structure prediction, are consistent with a model of PLB composed of a transmembrane helix (residues 33-52), a cytoplasmic helix (most likely residues 8-20), a β-sheet between residues 22 and 32, as well as a random coil at the N-terminus of the protein.

M-PM-D2

STRUCTURAL ORGANIZATION OF THE PENTAMERIC TRANSMEMBRANE α-HELICES OF PHOSPHOLAMBAN, A CARDIAC ION CHANNEL

Isaiah T. Arkin[1], Paul D. Adams[2], Kevin R. MacKenzie[2], Mark A. Lemmon[2,4], Axel T. Brünger[2,3] and Donald M. Engelman[2,5]

Dept. of [1]Cell.Biology, [2]Molecular Biophysics and Biochemistry and [3]Howard Hughes Medical Institute, Yale Univ. School of Medicine, New Haven, CT, USA [4]Present address: Dept. of Pharmacology NY Univ. Medical Ctr, NY, NY, USA

Phospholamban is a 52 amino acid calcium regulatory protein found as pentamers in cardiac SR membranes. The pentamers form through interactions between its transmembrane domains, and are stable in SDS. We have employed a saturation mutagenesis approach to study the detailed interactions between the transmembrane segments, using a chimeric protein construct in which staphylococcal nuclease is fused to the N-terminus of phospholamban. The chimera forms pentamers observable in SDS-PAGE, allowing the effects of mutations upon the oligomeric association to be determined by electrophoresis. Disruptive amino acid substitutions in the transmembrane domain lined up on faces of a 3.5 amino acids/turn helical projection, allowing the construction of a model of the interacting surfaces in which the helices are associated in a left-handed pentameric coiled-coil configuration. Molecular modeling simulations confirm that the helices readily form a left-handed coiled-coil helical bundle and have yielded molecular models for the interacting surfaces, the best of which is identical to that predicted by the mutagenesis. Residues lining the pore show considerable structural sensitivity to mutation, indicating that care must be taken in interpreting the results of mutagenesis studies of channels. The cylindrical ion pore (minimal diameter of 2 Å) appears to be defined largely by hydrophobic residues (I40, L43 and I47) with only two mildly polar elements contributed by sulfurs in residues C36 and M50.

M-PM-D3

ON THE NATURE OF THE UNFOLDED INTERMEDIATE IN THE *IN VITRO* TRANSITION OF THE COLICIN E1 CHANNEL DOMAIN FROM THE AQUEOUS TO THE MEMBRANE PHASE.

((S.L. Schendel and W.A. Cramer)) Dept. of Biol. Sci. Purdue University, West Lafayette, IN 47907.

The transition of the colicin E1 channel polypeptide from a water-soluble to membrane-bound state occurs *in vitro* at acid pH values that are associated with an unfolded channel structure whose properties qualitatively resemble those of a 'molten globule', or 'compact unfolded', intermediate state. The role of such a state for activity was tested by comparing the pH dependence of channel-induced solute efflux and the amplitude of the near-UV circular dichroism spectrum. The requirement of a partly unfolded state for activity was shown by the coincidence of the onset of channel activity, measured for membranes of four different lipid compositions, with the decrease in near-UV CD amplitude as a function of pH. Tertiary constraints on the three tryptophans of the colicin channel, assayed by the amplitude of the near-UV CD spectrum, are retained over the pH range 3–4 where channel activity could be measured and, as well, at pH 2. In addition, the tryptophan fluorescence emission spectrum is virtually unchanged over the pH range 2–6. The temperature independence of the near-UV spectrum at pH 3–6 up to 70° implies that the colicin E1 channel polypeptide is more stable than that of colicin A. A transition between 53–58 °C in the amplitude of the near-UV CD is consistent with preservation of part of the hydrophobic core in a destabilized state at pH 2. Thus, the unfolded state associated with colicin activity at acidic pH has the properties of a 'compact unfolded' state, having some, but not all of the properties of a 'molten globule'.

The small effect on local membrane acidity of a physiological acidic membrane lipid content, the retention of significant near-UV CD amplitude down to pH 2, and the small extent of immersion of the 40 Å globular colicin channel polypeptide in the 10 Å lower pH layer at the membrane surface, make it unlikely that a lower pH localized at the membrane surface significantly facilitates formation of an unfolded intermediate. (NIH GM-18457)

M-PM-D4

STRUCTURE OF THE OPEN AND CLOSED COLICIN Ia CHANNEL.

((S. L. Slatin, K. S. Jakes, X.-Q. Qiu and A. Finkelstein)) Albert Einstein College of Medicine, Bronx NY. 10461.

Channel-forming colicins are water soluble bacterial proteins that form voltage-dependent channels in planar lipid bilayers. We recently showed that gating is accompanied by a major rearrangement of the membrane-bound form of the colicin Ia protein. Biotin-labeling experiments have identified a 31 amino acid long segment, on the upstream side of the 40 amino acid hydrophobic segment of the colicin, that is translocated across the membrane in conjunction with gating; residues in this segment can be detected on the *cis* side of the membrane in the closed state, and on the *trans* side in the open state (Nature (1994), 371, 158-161). We show here that the translocated region extends, in fact, for at least 52 amino acids, and probably more.

The hydrophobic segment, which forms a pair of helices in the soluble form of the analogous colicin A, has also been assumed to form a pair of transmembrane helices in the Ia channel. We report here experiments with a mutant colicin Ia biotinylated at residue 594, in the middle of the hydrophobic segment, which suggest that this segment, unlike the translocated segment, is already inserted into the membrane in the channel's closed state, in the absence of a transmembrane potential.

Our observations severely restrict the number of transmembrane helices that can be envisioned to contribute to the structure of the channel.

M-PM-D5

PORE KINETICS OF LIPID VESICLES BY THE TRANSIENT DEQUENCHING OF AN ENTRAPPED FLUORESCENT DYE.
((G. Schwarz and A. Arbuzova)) Department of Biophysical Chemistry, Biocenter of the University, CH 4056 Basel, Switzerland

We consider the fluorescence signal of a liposome encapsulated self-quenching fluorescent dye in the course of an efflux process that has been induced by a pore forming agent. This signal is composed of two contributions, arising from the actually released dye and from the rest still being retained inside the liposomes, respectively. While the former part is fully dequenched, the latter one will exhibit a quenching factor Q depending on time and on the mode of release which could be "all-or-none" or more gradual. The Q can be measured and then be used to evaluate the average dye content of the vesicles as it decreases in the course of the time t. A basic quantitative analysis of the underlying theoretical problem will be presented, assuming pore inactivation being subject to a first order reaction step. When applied to pertinent experimental data, the pore formation rate per liposome, $p(t)$, as well as the average dye retention factor ρ of a single pore (related to the pore lifetime) may be determined. We shall give a practical demonstration of the procedures using data measured with carboxyfluorescein loaded phosphatidylcholine liposomes to which the wasp venom peptide mastoparan X had been added.

M-PM-D6

NON-EQUILIBRIUM PHASE SEPARATION DYNAMICS AND DOMAIN FORMATION IN BINARY LIPID BILAYERS

Kent Jørgensen and Ole G. Mouritsen
Department of Physical Chemistry, The Technical University of Denmark Bldg. 206, DK-2800 Lyngby, Denmark, [e-mail: fymearn@vm.uni-c.dk]

The non-equilibrium dynamics of the phase-separation process in binary lipid bilayers composed of saturated phospholipids, such as $DC_{14}PC$-$DC_{18}PC$ and $DC_{12}PC$-$DC_{18}PC$, has been studied theoretically by means of computer simulation on a microscopic interaction model. Particular attention is paid to non-equilibrium effects on bilayer heterogeneity in terms of local and global lateral membrane organization. The results reveal that a sudden temperature change which takes the binary lipid bilayer from the fluid one-phase region into the gel-fluid phase-coexistence region leads to formation of a large number of small lipid domains which are slowly growing in time. The growth of the lipid domains, which is limited by long-range diffusion of the lipid molecules within the two-dimensional bilayer plane, may give rise to a highly heterogeneous percolative-like bilayer structure with a network of interfacial regions that have properties different from those of the bulk gel and fluid phases. The results suggest that non-equilibrium effects may regulate lipid-domain formation and lateral organization in lipid bilayer membranes on various length- and time-scales.

M-PM-D7

Non Lamellar Phases in the POPC/$C_{12}E_2$/^2H_2O System. ((S.S.Funari and G.Klose)) University Leipzig, Dept. of Physics, Linnéstr. 5, D-04103 Leipzig, Germany. (Spon. by K.Brandenburg)

The phase diagram shows on the water poor leg, at low lipid contents, an inverted micellar L_2 phase which changes into inverted hexagonal as the lipid concentration increases. More lipid leads to the formation of a gel phase. On the lipid poor leg one finds cubic phases of inverted bicontinuous V_2 type. Temperature variation has shown that at some concentration they reversibly evolve from Ia3d to Pn3m upon heating.

Finally, in the surfactant poor region one finds a lamellar phase with specific characteristics. The ^{31}P NMR spectra from the lipid molecules (POPC) are characteristic of L_α phase, while the ^2H NMR spectra from ^2H_2O do not show a Pake powder, instead they show an almost "triangular" shape.

The cubic phases follow an epitaxial relationship going from lamellar, at lower temperatures, to inverted rods in a cubic array at higher ones (Ia3d).

The transition from L_2 to inverted hexagonal can be considered an unidirectional evolution of the unitary micelles. The sequence of phases with increasing the water content follows a change from negative to positive curvature at the water interface of the molecular aggregates.

M-PM-D8

FABRICATION OF MICROTUBULES IN MONOLAYERS OF A POLYAMINE-CHOLESTEROL DERIVATIVE.
((Fatemeh Mojtabai[1,2], Slawomir S. Mielewczyk[1], and Kenneth J. Breslauer[1])) [1]Rutgers University, Department of Chemistry, Piscataway, New Jersey 308855, and [2]Ultrathin Film Technology Route 46, Suite 310, Parsippany, New Jersey 07054.

Fabrication of materials with specific morphological structures and chemical characteristics is of particular interest in biotechnological applications. As part of an effort to develop anti-sense/gene diagnostics and therapeutics, we have synthesized a compound that can bind to nucleic acids and under specific conditions, form a tubular matrix. We have developed a new technique that allows us to fabricate tubules of a polyamine-cholesterol derivative at an air-water interface. We synthesized this compound by reacting cholesteryl chloroformate with spermine, followed by crystallization of the product. The crystals were dissolved in chloroform and spread at an air-aqueous buffer interface on a microscope-mountable monolayer trough. The monolayer was doped with a small amount of a fluorescent cholesterol analog, NBD-cholesterol. Our fluorescence microscopic imaging of the monolayer reveals information about the formation of tubules at the air-water interface upon compression of the monolayer from an expanded to a collapsed phase. The tubules have fairly thin walls and range from a few to hundred microns in diameter, with variable lengths that can be as long as several millimeters. We are exploring better control of the size and shape of the tubules by changing the rate of compression, temperature, pH and the ionic composition of the subphase.

M-PM-D9

FABRICATION AND FLUORESCENCE IMAGING OF HELICAL & TUBULAR MICROSTRUCTURES FROM MONOLAYERS OF A DIACETYLENIC PHOSPHOLIPID.
((Fatemeh Mojtabai,[1,2] and Kenneth J. Breslauer[1])) [1]Department of Chemistry, Rutgers University, Piscataway, New Jersey 08855, and [2]Ultrathin Film Technology, 2001 Route 46, Suite 310, Parsippany, New Jersey 07054).

We demonstrate a new, simple, and versatile technique for fabricating helical and tubular microstructures from diacetylenic lipids. The technique can be applied to the formation of other tubule forming amphiphiles as well. Specifically, the technique involves spreading monolayers of the lipid at an air-aqueous interface of a monolayer trough. Fluorescence microscopy is used to visualize formation of the monolayer and the tubules by probing the membrane with a fluorescent drug, daunomycin. The daunomycin provides a high contrast between the expanded phase and the condensed phase of the monolayer. Imaging of the membranes by laser-fluorescence microscopy reveals the typical feather-like domains of the diacetylenic lipid at the air-water interface, as well as a variety of other morphological structures, such as fibers, and tubules, which mostly appear at the bottom of the trough. The pitch length of the helical microstructures can be determined by observing changes in the fluorescence emission signal of the probe. Our preliminary analyses indicate that the size of the tubules and their pitch depend on the spreading conditions. For example, the size of the tubules appears to be more uniform in monolayers spread from a solvent than in monolayers made of vesicle preparations. We now are using electron microscopy and fluorescence imaging techniques to examine further these interesting observations.

M-PM-E1

STRUCTURAL ORGANIZATION OF THE BACTERIAL FLAGELLAR ROTARY MOTOR DETERMINED BY DIFFERENCE IMAGE ANALYSIS ((Dennis Thomas, Noreen R. Francis, Gina E. Sosinsky and David J. DeRosier.)) Rosenstiel Basic Medical Sciences Research Center, Brandeis University, Waltham, MA 02254.

The organelle of motility in *Salmonella typhimurium* is the bacterial flagellum. It is driven by a rotary motor at its base in the cell membrane. A proton gradient across the membrane provides the energy for rotation. A complex of two proteins MotA, the proton channel, and MotB, which interacts with MotA and the cell wall, form the stator portion of the motor. The motors, as imaged by electron cryo-microscopy, consist of the hook, L and P-rings(bushing), rod(drive shaft), MS-ring(rotor) and a large ring complex (the C-ring) located on the cytoplasmic face of the M ring. This large structure contains 12 different known proteins and has a MW of about 15 MD. Genetic analysis has shown that three proteins found in this structure, FliG, FliM and FliN, are involved in torque generation and control the direction of rotation. FliG is found in the membrane spanning MS ring complex which is part of the rotor. Immunomicroscopy data results suggest that FliM and FliN are located in the C ring. We have determined the structures of complete motors and motors partially stripped by varying preparative conditions. We also have prepared functional motors from gene fusion mutants which contain covalently linked switch/basal body proteins. Image analysis has revealed features not yet assigned to known proteins. We hope to identify the unknown proteins present and determine whether the C-ring is part of the rotor or stator of the motor.

M-PM-E2

STRUCTURAL STUDY OF THE *SALMONELLA TYPHIMURIUM* HOOK ((D.G. Morgan D.R. Thomas T.R. Shaikh and D.J. DeRosier)) Brandeis University, Waltham MA 02254-9110

Salmonella typhimurium flagella are composed of three major components: a rotary motor (the basal body complex with its associated proteins), a flexible universal joint (the hook) and a rigid propeller (the filament). The hook and filament, along with the rod portion of the basal body, form a continuous helical structure. We have recently determined the structure of flagellar filaments using electron microscopy and image analysis. Flagellin has a large outer domain (corresponding to amino acids in the middle of the sequence), a middle domain (comprised of sequences which flank those of the outer domain) and an inner domain (formed from the 70 N- and 30 C-terminal residues). Our 11 Å map of the filament indicates that the inner domain is a pair of concentric tubes whose walls are formed by columns of α-helices stacked end-to-end. The helical lattice of the hook is almost identical to that of the filament and our previous structural studies of the hook have shown a similar organization: an outer domain (likely formed from the middle of the sequence), a middle domain and an inner domain. However, details of the structure are lacking due to the low resolution nature (18-25 Å) of these studies. We have recently developed conditions where polyhooks can be efficiently straightened and prepared for electron microscopy by freezing in vitreous ice. This has made it possible to pursue higher resolution studies of these polyhooks. Our latest results are consistent with the model described above: the inner domain consists of a series of density rods aligned parallel to the hook axis and likely corresponds to axially oriented α-helices. We hope to extend the resolution of this work to beyond 10 Å, at which point we should be able to confirm the existence of these a-helices.

M-PM-E3

ATP-DEPENDENT WEAK INTERACTION BETWEEN CYTOPLASMIC DYNEIN AND MICROTUBULES. ((Zhaohui Wang and Michael P. Sheetz)) Department of Cell Biology, Duke University Medical Center, Durham, NC 27705. (Spon. by T. McIntosh)

Kinesin and cytoplasmic dynein convert the energy of ATP hydrolysis into mechanical force on microtubules. It was proposed that they alternate between strong and weak binding to microtubules during their force generating cycle. Following the movement of kinesin or cytoplasmic dynein-coated latex beads along microtubules, we can study the interactions between motor molecules and microtubules during force production. Kinesin and cytoplasmic dynein-coated beads exhibited three states on microtubules, stationary binding, active polar movement and diffusive movement. The mean square displacement vs. time plots of diffusing beads are linear, indicating Brownian diffusion (linear diffusion coefficient ~$6x10^{-10}$ cm^2/s). About 50% of the cytoplasmic dynein-coated beads which bound to microtubules diffused along microtubules whereas only a very small fraction of kinesin-coated beads (less than 1%) did. We also found that control beads lacking coated motors also bound and diffused on microtubules with similar frequency and diffusion coefficient as kinesin beads. The much higher fraction of cytoplasmic dynein-coated beads diffusing on microtubules is suggestive of a weak interaction between cytoplasmic dynein and microtubules. The percentage of diffusive beads coated with cytoplasmic dynein decreased in the absence of ATP, which suggests that the weak interaction is nucleotide-related and may represent a state of the motor during its force generation, for example, weak binding of cytoplasmic dynein to microtubules may represent a state that aligns the motor head for the next power stroke.

M-PM-E4

MECHANOCHEMICAL ASPECTS OF AXONEMAL DYNEIN ACTIVITY. ((T. Hamasaki, M.E.J. Holwill*, K. Barkalow and P. Satir)) Dept. of Anatomy & Structural Biology, Albert Einstein College of Medicine, Bronx, N.Y. 10461 and *Dept. of Physics, Kings College, London.

We have determined the relationship between microtubule length and translocation velocity from recordings of bovine brain microtubules translocating over a *Paramecium* 22S dynein substratum. In some samples, the 22S dynein has been subjected to detergent and/or to pretreatments that induce phosphorylation of the 29 kD light chain (Barkalow *et al*, 1994, J. Cell Biol. **126**:727-735). Control and treated dyneins have been used at the same densities in the translocation assays. In any given condition, translocation velocity shows an initial increase with microtubule length and then reaches a plateau. This is consistent with Michaelis-Menten kinetics, which we have used to interpret our data. The results indicate that the maximum translocation velocity (v_o), determined from a Lineweaver-Burk analysis, is increased by pretreatment, while the length constant (K_L), which corresponds to K_m, does not change with pretreatment, implying that the mechanochemical properties of the pretreated dyneins differ from control dyneins and permitting us to rule out the possibility that the velocity changes seen are caused by changes in geometry in the translocation assays or by the numbers of dyneins or dynein-heads needed to produce maximal translocational velocity. From our analysis, we also determine that *f*, the fraction of cycle time during which the dynein is in the force-generating state, is small - roughly 0.01, comparable to the *f* for HMM.

M-PM-E5

EVIDENCE THAT DIMERIZATION OF KINESIN HEAVY CHAIN INVOLVES STRUCTURES DISTINCT FROM THE KINESIN ROD. ((E.C. Young, E. Berliner*, H.K. Mahtani, B. Perez-Ramirez, and J. Gelles)) Biochemistry Dept. and *Biophysics Prgm., Brandeis University, Waltham MA 02254-9110.

The heavy chain (HC) of the *Drosophila* motor enzyme kinesin has heptad repeats beginning at approximately residue 437, which form a two-stranded α-helical coiled-coil in the "rod" domain observed by electron microscopy. Yang *et al.* [(1989) *Cell* **56**, 879-889] predicted that an HC fragment lacking the repeat would form a monomer corresponding to one of the two "heads" observed at one end of the rod. To test this prediction, we expressed in insect cells two HC chimeras: K448-BIO contains the 448 N-terminal residues of HC fused at the C-terminus to a two-residue linker and a C-terminal fragment from *E. coli* biotin carboxyl carrier protein; K448-L is the same except it contains only the HC and linker residues. Both chimeras, like kinesin, are ATPases activated by microtubules (MTs); K448-BIO displays MT motility. Equilibrium sedimentation, gel filtration, and SDS-PAGE show that purified K448-BIO and K448-L at 0.02-0.4 mg/mL form homogeneous solutions of non-covalent homodimers (association constant $\geq 2 \times 10^8$ M^{-1}), with no detectable monomers or higher order oligomers. The algorithm of Lupas *et al.* [(1991) *Science* **252**, 1162-1164] predicts the chimeras lack the HC's long coiled-coil, and thus structures responsible for chimera dimerization are distinct from kinesin rod. Such structures might serve to prevent simultaneous binding of both heads to the MT in some kinesin reaction cycle intermediate.

M-PM-E6

Kinetic Mechanism of Microtubule-Kinesin ATPase Motor Domain K560 Y.Z. Ma and E.W. Taylor Dept. of Mol.Gen., Univ. of Chicago, Chicago, Il 60637

Human kinesin K560 dimer, which contains part of the coiled-coil region and moves microtubules, was compared with K379 motor domain which can also form dimers.Both proteins showed the same steps in the kinetic scheme but most of the rate constants for K560 were smaller than those for K379. Binding of fluorescent substrate analogues, methylanthranyloyl ATP (mant-ATP) and mant ADP gave a fluorescence increase signal followed by fluorescence decrease signal, which indicates that two isomerizations are induced by nucleotide binding. The maximum rate for the fluorescence increase measures an isomerization step which is 150 s^{-1} for K560 and 200 s^{-1} for K379. The rate of the ATP hydrolysis step is 60-70 s^{-1} for microtubule-K560 and 100 s^{-1} for microtubule-K379 compared to 7-10 s^{-1} for kinesin alone. The steady state ATPases of both K560 and K379 were activated about 3000 fold by microtubules with $K_{0.5(microtubule)}$ of 2.2 μM and k_{cat} equal to 15 s^{-1} for microtubule-K560 and 25 s^{-1} for microtubule-K379. The rate constants of ADP dissociation for kinesins alone and microtubule-kinesins were similar to the steady state ATPases thus ADP dissociation is a rate limiting step. These results suggested that the conformation of K560 is more constrained than that of K379. The microtubule-kinesin dimer-ADP complexes released one ADP per dimer at approximately the steady state turnover rate but the second ADP was released slowly(1 to 3 s^{-1}) similar to the results of Hackney(PNAS 1994.91.6865). Binding of nucleotides(ATP,GTP,AMPPNP) to available nucleotide sites increased the rate of dissociation of the second ADP but at different rates (120 s^{-1} for ATP). The relation of kinetic mechanism to motility is discussed.

M-PM-E7

THE ISOMETRIC FORCE OF A SINGLE KINESIN MOLECULE. ((C.M. Coppin*, J.T. Finer#, J.A. Spudich# and R.D. Vale*$^))) Departments of *Pharmacology and $Biochemistry, University of California, San Francisco, CA 94143; ^ The Marine Biological Laboratory, Woods Hole, MA 02543; #Departments of Biochemistry and Developmental Biology, Beckman Center, Stanford University School of Medicine, Stanford, CA 94305

The displacements and isometric forces produced by a single kinesin molecule translocating along a stationary axoneme were measured using the optical trap feedback apparatus of Finer et. al. (Finer, J. T. et al. Nature 368: 113-119, 1994). As a kinesin-bound bead moved up the force gradient of the optical trap, it usually exhibited discrete displacements of approximately 8 nm, similar to those described by Svoboda et al. (Svoboda, K. et al. Nature 365: 721-727, 1993). Frequently, the kinesin could move the bead against forces of about 3-5 pN before it released from the microtubule and returned to the trap center. The steps were separated by pauses ranging in duration from a few milliseconds to more than two seconds. A statistical analysis of all the observed pauses is under way.

When the position of the bead was clamped by feedback control of the optical trap's position, kinesin consistently achieved somewhat greater maximal forces than during translocation of the bead. Unlike myosin, which exhibits single force transients, kinesin reached its maximal force in a discontinuous fashion. At 20 μM ATP, the maximal force was often sustained for long periods lasting up to several seconds, but the force transient was sometimes abruptly terminated much sooner. This apparatus is currently being used to further define the characteristics of kinesin's force-generating and elastic components.

M-PM-E8

THE FORCE GENERATED BY A SINGLE KINESIN MOLECULE AGAINST AN ELASTIC LOAD ((E. Meyhöfer and J. Howard)) Dept. of Physiology and Biophysics, University of Washington, Seattle, WA 98195 and Klinische Physiologie, Medizinische Hochschule Hannover, 30623 Hannover, FRG.

To probe the molecular mechanism of force generation we used the kinesin *in vitro* motility assay as a model system and measusured the force single motor molecules can exert against microtubules.We developed a measurement technique that uses tiny glass fibers of calibrated stiffness as force transducers. One end of a biotinylated microtubule is attached via strepavidin to the tip of the glass fiber, the other end is allowed to interact with the surface of a small silica bead sparsely coated with kinesin. The tip of the glass needle is imaged onto a photodiode detector to track the displacements of the microtubule by kinesin with a spatial and force resolution of 1 nm and 1 pN respectively. Fibers were calibrated from the thermal motions of their tips. Their stiffnesses ranged from 0.02 to 0.63 pN/nm. The temporal resolution of the recordings was limited by the time constant of the fibers (0.33 - 5.7 ms).

At low kinesin density we observed stereotyped interactions between motors and microtubules: the speed was initially high, close to the unloaded gliding velocity, and decreased approximately linearly as the maximum force was reached. The repeatability of the events, the low kinesin density (at most 0.5 - 3 kinesin molecules on the surface of the sphere could interact with the microtubule) and the consistent forces (range 4 - 8 pN) suggest that the measurements were from single motors.The maximum force was 5.4 ± 1.0 pN (mean ± SD, n = 16), independent of the stiffness of the fiber, the damping from the fluid, and on whether or not the ATP concentration was high or low.

Supported by the Washington Affiliate of the AHA (EM), and NIH (AR40593) and Pew grants to JH.

K^+ CHANNELS I

M-Pos1

FIXED CHARGE SUBSTITUTION IN K_{Ca} CHANNELS. ((A. Lagrutta, K.-Z. Shen*, R.A. North**, and J.P. Adelman)) Vollum Institute for Advanced Biomedical Research, Oregon Health Sciences University, Portland, OR 97201.

Slowpoke is a large conductance, calcium-activated potassium channel cloned from *Drosophila*. Two glutamate residues in the carboxy terminal portion of transmembrane domain 6 were neutralized (EE335,338QQ) or reversed in charge (EE335,338KK). The double charge neutralization gave a complex phenotype, as analyzed in inside-out patches from *Xenopus* oocytes ($[K^+]_o = [K^+]_i$ = 120 mM; $[Mg^{2+}]_i$ = 2 mM; $[Ca^{2+}]_o$ = 1.8 mM). We determined mean unit currents in single and multi-channel (2-5) patches using all-point amplitude histograms, and then looked at the statistical distribution of these unit currents. Several current levels lower than wildtype were detected at all potentials tested. At +100 mV, these levels were 13.57 ± .34 (n = 4), 11.30 ± .14 (n = 11), 8 ± .14 (n = 17), and 5.35 ± .26 (n = 5) pA, while wildtype unit current was 14.93 ± .13 (n = 8). In some patches that appeared to contain a single channel, 2 or more of these conductance levels were present, with each conductance exhibiting characteristic gating properties. These results suggest that glutamates 335 and 338 are not only contributing to the unit conductance of the open channel, but also to kinetic transitions. To further analyze this phenotype, we introduced point mutations at positions E335 and E338, neutralizing or reversing charge. The E335Q, E338Q and E338K mutants showed a single conductance level (153, 178, and 131 pS, respectively; wildtype conductance: 196 pS), while the E335K mutant displayed two levels (122 and 166 pS). In E335K single channel patches the conductance levels are best described as gating modes. Current work is assessing the mechanistic basis of these discrete conductance levels.

Supported by NIH grant NS31872.

* Current address: Dept. of Pharmacology, O.H.S.U., Portland, OR 97201.
** Current address: Glaxo Institute for Molecular Biology, Geneva, Switzerland.

M-Pos2

BARIUM BLOCKADE OF A CLONED Ca^{2+}- ACTIVATED K^+ CHANNEL (*hSlo*) EXPRESSED IN *XENOPUS LAEVIS* OOCYTES. ((F. Díaz§, M. Wallner*, E. Stefani*, L. Toro* and R. Latorre§)) *UCLA, Los Angeles, CA 90024. §CECS and Univ. Chile, Santiago 9, Chile.

We have expressed the high conductance Ca^{2+}-activated K^+ channel *(hSlo)*, cloned from human myometrium in *Xenopus laevis* oocytes. In cell-attached patches, depolarizing pulses to 100-180 mV elicit ionic currents that increase with time and afterwards remain at a constant value (do not "inactivate"). However, in excised inside-out macropatches, pulses to the same potentials elicit currents that "inactivate"; they increase to a maximum value and then decay with time constants (~200 ms) that become faster for larger depolarizations. Recovery from this process has a time constant of 3 s at 0 mV. The time-dependent current reduction was manifested in single channel records as long-lived closed states triggered by large depolarizations. Internal Ba^{2+} is able to block high conductance Ca^{2+} -activated K^+ channels with high affinity. Addition of a "crown ether" Ba^{2+} chelator ((+)-18-crown-6-tetra-carboxylic acid) to the cytoplasmic side, to a final concentration of 20 μM, removed almost all the current inhibition promoted by depolarizing pulses in the 100 to 180 mV range. The crown ether effect was reversible upon perfusion of the internal side of the macropatch with a crown ether-free solution. These results suggest that the current decay for large depolarizations, in excised patches, is due to contaminant Ba^{2+} in the solutions that blocks *hSlo* channels, and not to an intrinsic voltage-dependent inactivation process uncovered by patch excision. Supported by NIH HL47382, GM50550, Progr. Becas Doc. CONICYT, and FNI 1940227.

M-Pos3

ELECTROSTATIC CONTROL OF MAXI-K CHANNEL TOXIN SPECIFICITY. ((T.J. Mullmann[1],P. Munujos[2], M.L. Garcia[2] and K.M. Giangiacomo[1])) [1]Dept. of Biochemistry, Temple Medical School, Philadelphia, PA 19140 and [2]Dept. of Membrane Biochemistry & Biophysics, Merck Research Laboratories, Rahway, NJ 07065

Iberiotoxin (IbTX) and Noxiustoxin (NxTX) are both highly charged peptide toxins that block the maxi-K channel with high and low affinity, respectively. Electrostatic potential maps calculated from the 3-dimensional structure for IbTX and a model of the NxTX structure reveal striking differences in their distributions of charge that may control their binding specificity. To identify electrostatic elements of the toxin structures that control the rates of toxin association and dissociation, we have examined toxin block of single maxi-K channels incorporated into planar lipid bilayers. Toxin dissociation rates for IbTX and NxTX vary over 80,000-fold. The average duration for NxTX block of the maxi-K channel was ~10 ms (V_m=-20mV), compared to 840 sec for IbTX (V_m=40mV). Removal of positive charges at residues K27 and R34 in IbTX increased the toxin dissociation rates for IbTX 2- and 50- fold, respectively. The rates of association for NxTX and IbTX are differentially influenced by ionic strength. The association rate for NxTX decreased ~ 20-fold as external potassium was increased from 25 to 100 mM. In contrast, the IbTX association rate decreased 3.4-fold. A mutant of IbTX with no net charge, IbTXR34N, exhibited an ionic strength dependence of its association rate similar to that of wild type IbTX. These findings suggest that the rates of toxin association are controlled by the distribution of toxin charge rather than the net charge.

M-Pos4

CLONING OF A MAXI CA-ACTIVATED K-CHANNEL FROM BOVINE AORTIC SMOOTH MUSCLE: SENSITIVITY TO A KUNITZ INHIBITOR. ((G.W.J. Moss, J. Marshall, M. Morabito, E. G. Moczydlowski and J. Howe)) Dept. of Pharmacology, Yale Univ. School of Medicine, New Haven, CT 06520.

Aortic smooth muscle cells express a high density of maxi K(Ca) channels. Previous results have shown that such K(Ca) channels have an internal binding site for Kunitz-type protease inhibitors and dendrotoxins which mediates production of discrete subconductance events in single channels. To study this peptide-channel interaction, the alpha subunit of a K-channel homologous to the *Drosophila slowpoke* K(Ca) channel was cloned from cultured bovine aortic smooth muscle cells. Except for alternatively spliced regions, the deduced amino acid sequence of the cloned cDNA (denoted *bSlo*) is >99% identical to the mouse *mSlo* K(Ca) channel reported by Butler et al. (1993). The isolated *bSlo* clone lacks alternatively spliced insertions A and B previously described in *mSlo* (Butler et al. 1993). *bSlo* also differs from *mSlo* at the C-terminus: 61 C-terminal residues in *mSlo* are replaced by a different 8-residue sequence in *bSlo*. This latter difference may represent a third splicing site that is functionally significant in smooth muscle. The *bSlo* clone was transiently expressed by transfection into cultured human embryonic kidney cells (HEK293) and K(Ca) channels were recorded by the patch clamp technique. The expressed channel exhibits many of the properties of the native channel in vascular smooth muscle including a unitary conductance of ~250 pS in symmetrical 150 mM KCl. To determine whether this cloned K(Ca) channel alpha subunit contains the binding site for Kunitz inhibitors, BPTI (bovine pancreatic trypsin inhibitor) was applied to the intracellular side of expressed channels. BPTI was found to induce subconductance events characteristic of the native channel in smooth muscle cells. This result indicates that the channel-forming alpha subunit of maxi K(Ca) channels contains the internal binding site for BPTI and dendrotoxins. (Supported by Donaghue Foundation, AHA, NIH.)